EVS26
Los Angeles, California, May 6 - 9, 2012

Parameterization of Electrical Battery Model for Use in Dynamic Simulations of Electric Vehicles

Ari Hentunen[1], Teemu Lehmuspelto[2], Jussi Suomela[3]
[1]*Aalto University, Department of Electrical Engineering*
Puumiehenkuja 5 A, 02150 Espoo, Finland, ari.hentunen@aalto.fi
[2]*Aalto University, Department of Engineering Design and Production*
Puumiehenkuja 5 A, 02150 Espoo, Finland, teemu.lehmuspelto@aalto.fi
[3]*Aalto University, Department of Automation and Systems Technology*
Otaniementie 17, 02150 Espoo, Finland, jussi.suomela@aalto.fi

Abstract

During the development of electric vehicles and non-road mobile machinery, dynamic system-level simulations are utilized to validate the design and the sizing of components as well as to validate the control software. The model needs to predict e.g. the open-circuit voltage, terminal voltage, and state-of-charge under various load profiles. Electrical battery models are commonly used, because they are simple and computationally relatively light but still provide good accuracy. Despite the simplicity and low number of parameters, the complex behavior of electrochemical batteries still make the parameter extraction a tedious process. The problematic nature of the parameters to depend on the state-of-charge, temperature, current-rate, current-direction, and aging causes challenges in the parameterization. This paper describes and demonstrates the model parameter extraction process for a Thevenin-based electrical model, and presents a set of experiments and a methodology to extract the parameters. A commercial lithium-manganese-nickel-cobalt-oxide battery module is used in the experiments.

Keywords: battery model, modeling, simulation, EV, off-road

1 Introduction

The multidisciplinary nature of batteries has led to many different kinds of modeling approaches, which can be generally divided into electrochemical, mathematical, and electrical modeling. For system-level simulation of *electric vehicles* (EVs), electrical models are commonly used [1], because they are fast to execute, simple and intuitive to analyze, and provide accurate *state-of-charge* (SOC) and *open-circuit voltage* (OCV) prediction. The model can rather easily be augmented to predict also e.g. the state-of-health and temperature, which are often needed in the simulations. Parameter extraction of electrical models can be done with simple experiments without any need of battery-specific proprietary information of the used materials.

Electrical models are *electrical equivalent circuits* (EECs) that mimic battery's electrical behavior, e.g., steady-state voltage, OCV, and transient voltage. Electrical equivalent circuits are typically combinations of electrical sources, resistors, capacitors, and inductors. For electrical engineers electrical models are very handy and intuitive, and those models can be easily used in circuit simulators and other system simulators. The accuracy of electrical models is good, the percentual error is usually in the order of few percents.

Lots of electrical battery models for different battery chemistries have been developed. Generally, for system-level dynamic simulations of EVs, usually Thevenin-based or impedance-based models are used. Thevenin-based models are typically parameterized based on some sort

of *current-pulse* (CP) experiments [2–5], while the parameter extraction of the impedance-based models rely on *electrochemical impedance spectroscopy* (EIS) measurements at different operating points. For the EIS methodology, the time to make the impedance measurements take long, and also a frequency analyzer is needed to perform the tests. For the CP tests, programmable power supply and load are needed accompanied with extensive data logging, temperature sense, and measurement of electrical quantities such as current, voltage, and ampere-hours. The basic experiments at the typical temperature and current-rate can be done quite fast, but if the temperature and current-rate effects need to be extracted also, the duration of the tests increase significantly.

This paper represents a Thevenin-based electrical battery model, and describes the parameter extraction process for the model. Parameter extraction is based on *pulse-discharge* (PD) and *pulse-charge* (PC) experiments, which are sequences of CP experiments with a rest-time between consecutive current pulses. Also the general picture of the inclusion of temperature, current-rate, and aging effects is covered.

The rest of the paper is organized as follows. In section 2, the model structure and dynamic analysis of the model are explained in detail. The model parameter extraction is covered theoretically in section 3 and experimentally in section 4. Section 4 covers also the model validation. Section 5 concludes the paper.

2 Model

The EEC of a battery is shown in Fig. 1, where u_{oc} is the open-circuit voltage, u_{b} is the terminal voltage, i_{b} is the terminal current, R_0 is the ohmic DC resistance, $R_1, R_2, \ldots, R_n$ are the dynamic resistances, and $C_1, C_2, \ldots, C_n$ are the corresponding dynamic capacitances. All resistances and capacitances are functions of the SOC, temperature, current-rate, current-direction, calendar life, and cycle life.

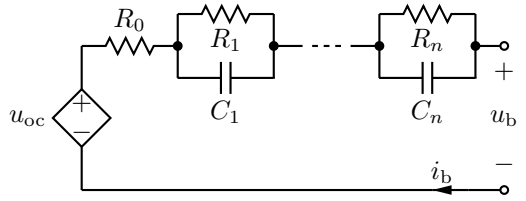

Figure 1: Electrical equivalent circuit.

What is not explicitly shown in the EEC is that also the SOC is predicted by the model, and that the self-discharge behavior is included in the SOC prediction. The controlled voltage-source then provides the predicted OCV as a function of SOC. Generally, also temperature-dependency and charge/discharge-history dependency can be included into the OCV prediction. By representing the OCV as a function of SOC only, the prediction is simplified and the OCV can be represented e.g. as a *lookup table* (LUT) or as a mathematical expression, e.g. a polynomial function.

2.1 Usable capacity

The usable capacity Q_{us} is expressed as follows:

$$Q_{\mathrm{us}}(N, t_{\mathrm{y}}, T) = Q_{\mathrm{n}} \times f_1(N) \times f_2(t_{\mathrm{y}}) \times f_3(T) \tag{1}$$

where Q_{n} is the nominal capacity in $\mathrm{A{\cdot}s}$, N is the cycle number, T is the temperature, t_{y} is the time in years, $f_1(N)$ is the cycle-dependent correction factor, $f_2(t_y)$ is the calendar-time dependent correction factor, and $f_3(T)$ is the temperature-dependent correction factor. Battery manufacturers usually have some information about the cycle-life and calendar-life aging that can be used as a basis for the correction factors $f_1(N)$ and $f_2(t_{\mathrm{y}})$. Manufacturers also usually have a graph about the discharge and charge curves at different temperatures that can be used as a basis for the temperature-dependent correction factor $f_3(T)$. It is also relatively easy to obtain it experimentally, if isothermal conditions can be provided.

2.2 State of charge

The SOC is predicted by coulomb counting:

$$s_Q = s_{Q_0} - \frac{1}{Q_{\mathrm{us}}} \int (i_{\mathrm{b}} + i_{\mathrm{sd}})\, \mathrm{d}t \tag{2}$$

where s_Q is the SOC, s_{Q_0} is the initial SOC, and i_{sd} is the self-discharge current. The self-discharge characteristics may be obtained experimentally, and based on the experiment, the equivalent self-discharge current i_{sd} may be obtained.

2.3 Open-circuit voltage

The nonlinear relation between the SOC and OCV is represented as a controlled voltage source $u_{\mathrm{oc}}(s_Q)$. The relation can be obtained from experimental tests. It is usually sufficient to represent the OCV as a function SOC only.

2.4 Transient response

Under loading the terminal voltage differs from the OCV. In the model, resistor R_0 represents the battery's electronic resistance, i.e. the ohmic resistance, which encompasses the resistivity of the actual materials such as metal plates and contact resistances. The dynamic resistances $R_1 \ldots R_n$ represent the ionic resistances, which are caused by various electrochemical factors such as electrolyte conductivity, ion mobility, and electrode surface area. These polarization effects happen more slowly than the effect of electronic resistance, which is instantenous. This slowly increasing effect is modeled as parallel capacitances $C_1 \ldots C_n$.

Because there are many electrochemical reactions that occur at different time scales, the number of RC-branches depends on the desired accuracy of the model. A comprehensive analysis of the selection of proper number of RC branches can be found in [6]. As a summary, the choice of number of RC networks is a compromise between accuracy and computational complexity, the latter being more of an issue if the model is changed into an online model that is executed in a real-time application such as a BMS. In [6], it was shown that after two RC branches, the accuracy increments get small compared to the exponentially increasing computational complexity. Usually, one to three branches are used, two being a good compromise.

2.5 Dynamic analysis

Consider the equivalent circuit of Fig. 1 with n RC branches. The following equations describe the dynamic behavior:

$$\frac{\mathrm{d}}{\mathrm{d}t}u_i = \frac{1}{C_i}i_\mathrm{b} - \frac{1}{R_i C_i}u_i\,,\ \ i = 1, 2, \ldots, n \quad (3)$$

$$u_\mathrm{b} = u_\mathrm{oc} - R_0 i_\mathrm{b} - u_1 - u_2 - \ldots - u_n \quad (4)$$

These equations can be formulated in state-space representation:

$$\dot{\mathbf{x}} = \mathbf{A}\mathbf{x} + \mathbf{B}\mathbf{u} \quad (5)$$

$$y = \mathbf{C}\mathbf{x} + \mathbf{D}\mathbf{u} \quad (6)$$

where

$$\mathbf{x} = \begin{bmatrix} u_1 & u_2 & \cdots & u_n \end{bmatrix}^\mathrm{T}$$

$$\mathbf{u} = \begin{bmatrix} u_\mathrm{oc} & i_\mathrm{b} \end{bmatrix}^\mathrm{T}, \quad y = u_\mathrm{b}$$

$$\mathbf{A} = \begin{bmatrix} -\dfrac{1}{R_1 C_1} & 0 & \cdots & 0 \\ 0 & -\dfrac{1}{R_2 C_2} & \cdots & 0 \\ \vdots & \vdots & \ddots & \vdots \\ 0 & 0 & \cdots & -\dfrac{1}{R_n C_n} \end{bmatrix}$$

$$\mathbf{B} = \begin{bmatrix} 0 & 0 & \cdots & 0 \\ \dfrac{1}{C_1} & \dfrac{1}{C_2} & \cdots & \dfrac{1}{C_n} \end{bmatrix}^\mathrm{T}$$

$$\mathbf{C} = \begin{bmatrix} -1 & -1 & \cdots & -1 \end{bmatrix}, \quad \mathbf{D} = \begin{bmatrix} 1 & -R_0 \end{bmatrix}$$

State-space representation can be transformed to transfer-function representation by Laplace-transformation and solving $\mathbf{x}$ and then substituting it to (6):

$$\mathbf{x}(\mathrm{s}) = (\mathrm{s}\mathbf{I} - \mathbf{A})^{-1}\,\mathbf{B}\mathbf{u}(\mathrm{s}) \quad (7)$$

$$y(\mathrm{s}) = \left[\mathbf{C}\,(\mathrm{s}\mathbf{I} - \mathbf{A})^{-1}\,\mathbf{B} + \mathbf{D}\right]\mathbf{u}(\mathrm{s}) \quad (8)$$

where $\mathbf{\Phi}(\mathrm{s})$ is state-transition matrix. Input-to-state and input-to-output transfer functions can then be expressed as

$$\frac{\mathbf{x}(\mathrm{s})}{\mathbf{u}(\mathrm{s})} = \mathbf{\Phi}(\mathrm{s})\mathbf{B} \quad (9)$$

$$\frac{\mathbf{y}(\mathrm{s})}{\mathbf{u}(\mathrm{s})} = \mathbf{C}\mathbf{\Phi}(\mathrm{s})\mathbf{B} + \mathbf{D} \quad (10)$$

2.6 Curve-fitting methodologies

The OCV as well as the resistors and capacitors of the transient response RC network are functions of SOC. The easiest method to implement their characteristics is to represent them with LUTs and utilizing linear interpolation between data points. Another possibility is to utilize curve-fitting techniques [7] and to represent the characteristics as mathematical functions. For example, the OCV can be represented with a polynomial

$$f(x) = p_0 + p_1\,x + p_2\,x^2 + \ldots + p_n\,x^n \quad (11)$$

where n is the degree of the polynomial, constants p_0 to p_n are the corresponding constants from the fitted curve, and x is the variable, i.e., SOC. Exponential fit may be useful for functions that exhibit exponential growth or decay:

$$f(x) = a_1\,e^{b_1 \cdot x} + a_2\,e^{b_2 \cdot x} + \ldots + a_n\,e^{b_n \cdot x} \quad (12)$$

where n is the number of exponential terms, a_n and b_n are the corresponding constants from the fitted curve, and x is the variable, e.g., SOC. As will be seen later, the characteristics of the EEC's resistances are similar to an exponential function, and hence, exponential functions are often well-suitable to characterize the resistances.

2.7 Cycle-life and calendar-life effects

The cycle-dependent correction factor $f_1(N)$ in (1) can be implemented e.g. as a LUT or a polynomial function, if the relation between the cycle number and the capacity is known accurately. If there is no exact information available other than cycle life at 80 % DOD, a linear polynomial can be used as a first approximation:

$$f_1(N) = 1 - \frac{0.2}{N_\mathrm{nom}} \times N \quad (13)$$

where N_nom is the nominal cycle life of the battery.
In hybrid vehicles, the battery is usually never fully charged or discharged. Instead, the loading profile consists of repetitive short-time charging and discharging pulses. Consequently, the SOC

is usually kept in a small area around some operating point, e.g. 50 %. These shallow cycles need to be converted to full cycles for the function f_1. If there is no better knowledge available, it is possible to convert the nominal cycle life value to ampere-hours and to integrate the charge or discharge current to get the actual cumulative ampere-hour value of the battery. One cycle is then equal to 80 % of the nominal capacity of a fresh battery, e.g. for a 10 Ah battery, one cycle is achieved when 8 Ah is discharged from the battery in total. Discharging need not be continous, and there may be charge intervals in between.
The calendar-life correction factor $f_2(t_y)$ can be implemented in the same way as the cycle-life correction factor.

$$f_2(t_y) = 1 - p_1\, t_y \tag{14}$$

where p_1 is the slope of the curve. However, battery specification does not usually give any information about the calendar life.
Aging increases also the ohmic and ionic resistances. Therefore, LUTs can be added that increase the resistance values as a function of aging.

2.8 Temperature effects

Function $f_3(T)$ can be determined from experiments at different temperatures, or from manufacturer's datasheet, which usually includes charge and discharge curves with relative capacity at different temperatures. Lower temperatures increase cell impedance due to diffusion kinetics. The function f_3 can also be slightly larger than one at elevated temperatures. A linear mapping can be presented as

$$f_3(T) = 1 + p_1\,(T - T_0) \tag{15}$$

where p_1 is the slope of the curve, T is the temperature in °C, and T_0 is the normal temperature, where the temperature-correction factor is unity.
Temperature affects also the ohmic and ionic resistances. Therefore, LUTs can be added that increase or decrease the resistance values as a function of temperature. It is also possible to obtain experimentally directly a multidimensional map instead of 1D-map, if the experiments for the parameter extraction are made at several constant temperatures in a temperature chamber. Then, the resistance and capacitance values vary as function of SOC and temperature.

2.9 Current-rate effects

The current rate affects the resistance and capacitance values of the model. As the current-rate increases, the resistance values decrease. The relation between the current-rate and the resistance values can be extracted from the PC and PD experiments. The function can be easily implemented in the model as a LUT, but also mathematical expressions can be used. It is also possible to include the current-rate effect directly into the resistance and capacitance mappings as an extra dimension, similarily as the temperature effect.

3 Model extraction

Model extraction is based on simple experimental tests that can be done in cell-level, module-level, or pack-level test environment.
The following characteristics need to be extracted for the model:

- Nominal capacity
- OCV mapping
- Ohmic resistance
- RC parallel branches
- Self-discharge behavior
- Temperature effect
- Current-rate effect
- Cycle-life and calendar-life effects
- Different characteristics during charging and discharging

The first four items are the most important ones and are necessary properties, which describe the characterics of a fresh battery in its nominal operating point. The rest of the items are more or less optional and can also be added later on.
A set of PD and PC experiments are used to reveal the capacity, SOC–OCV mapping, ohmic resistance values, and RC circuit network parameter values. Also current-rate effect can be deduced from the same experiments. In each experiment, a full battery is discharged with constant-current pulses, which are followed by rest periods. There are two purposes for the rest periods:

- to reveal the voltage relaxation characteristics, and consequently, the ohmic resistance, RC circuit parameters, and the OCV in case of OCV characterization experiment
- to let the battery temperature to cool down

To obtain best results, the internal temperature of the battery should stay constant during the experiments, i.e. isothermal conditions are preferred. This can be achieved by placing the battery into a thermal chamber, or by providing effective cooling, e.g. by using liquid-cooling plates between the cells.

3.1 Experimental test setup

A programmable electronic load and a charger are needed for battery characterization experiments. The current rating for the equipment should be high enough to provide the specified maximum current for loading and charging.
The sampling rate should be fast enough to catch the rapid voltage change caused by the ohmic resistance at the current pulse starting and ending time instants as well as the fast dynamics of the voltage response after that. The sampling rate for the ohmic resistance should be in the order of hundreds milliseconds. Also the fastest time constant of the equivalent circuit may be in the order

of seconds, and hence, there should be enough data points to fit the model parameters. On the other hand, the experiments are long, yielding to huge amount of data if very short sampling time is used. Therefore, a compromise between the amount of data and accuracy must be made.
Cell-level testing is the simplest and fastest approach to characterize batteries. Single cells are easy to order, deliver, and handle. Also the voltage rating of the electronic load and power supply are low, and therefore, the price of the equipment is low. In addition, no BMS or other auxiliary electronics is needed, which makes it easy to set up the experiment.
During the development of a full battery pack and vehicle control software, the BMS functionality must be tested in the laboratory. Therefore, a module-level test system is often needed anyway to test the BMS and vehicle control software. In addition, the module-level test environment gives information about the tolerances between the cells in a module, resulting in a more realistic model of the battery module compared to a model that is constructed using the number of series and parallel connected cells with the characteristics of the single cell that was tested. Module-level testing gives also information about the cooling needs of the battery module, which is of major importance when developing a battery system.
When moving into a pack-level testing, everything gets more complicated. First, pack-level electronic loads and power supplys are very expensive and big in volume and weight. Second, the full-scale batteries for EVs are expensive to obtain for evaluation purposes, and the delivery, handling, and setting up of the experiment are time-consuming procedures.
Temperature measurements from the surface of a cell are very important. Modules and packs usually have numerous temperature sensors inside them, and the data can be accessed from the BMS. In that case, the data from the BMS is enough, and that data should be combined with the other measurement data. Otherwise, temperature sensors should be attached inside the module or pack into the surface of cells.
In order to extract efficiently and accurately also the temperature-effects, a temperature chamber is needed. Otherwise, experiments at cold or hot temperatures cannot be made. In addition, liquid-cooling helps to keep the temperature constant during the experiment.

3.2 Model extraction

Generally, all model parameters—except the self-discharge behavior—can be extracted from the PD and PC experiments. However, also other experiments such as constant-current discharge may be used e.g. to determine the capacity or OCV. If the current-rate and temperature effects are neglected, the whole characterization can be made with one PD experiment followed by one PC experiment. Then, the characterization should be made with the typical current-rate of the application at the typical temperature.
The number of current pulses in PD and PC experiments is a compromise between the desired accuracy and duration of the experiment. Obviously, the duration increases with the pulses, because after each pulse a rest period is employed. With ten current pulses, i.e. 10 % SOC per pulse, the behavior of a battery can be characterized with good accuracy for dynamic simulation purposes. For example, with 10 % pulse-rate and 10 min rest period at 1C current-rate, the duration of the PD experiment becomes approximately 2 h 40 min. The accuracy can be increased by having more current pulses or longer rest periods. The lenght of the rest period can be selected arbitrarily. However, with very short rest periods the long time constant may not be extracted reliably nor accurately. On the other hand, with very long rest periods the duration of the experiment becomes long.
Before starting the characterization, the battery needs to be fully charged. If two or more cells are connected in series, the total available capacity is affected also by the charge balance as well as the differences of the cells. The weakest cell with the lowest capacity determines the maximum available capacity of the battery. That is why the BMS needs to first balance the battery, and only after that is done, the model extraction should be started.
Parameters of the equivalent circuit of Fig. 1 can be extracted by making a set of PD and PC experiments with several discharge rates. In each PD experiment, a full battery is discharged with constant-current pulses, which are followed by rest periods. Fig. 2 shows a typical PD experiment for a 40 Ah battery, where a full battery is pulse-discharged with 10 % pulses and 30 min rest time.

3.2.1 Capacity

Perhaps the simplest method for capacity extraction is to discharge a full battery at its nominal temperature with a low rate until the cut-off voltage is reached. The ampere-hours should be measured during the experiment, preferably with a power analyzer to get accurate result. If the battery consists of several cells, the discharging should be stopped when the first cell reaches the cut-off voltage. However, because the terminal voltage is affected by the internal resistance voltage drop and relaxation effect, there is still some charge left in the battery that can be extracted when the relaxation effect is over. The length of the relaxation effect is in the area of hours. Therefore, the discharging should be continued after a long rest period with a very low current. This procedure of slow-rate discharging and resting may be done several times to obtain the best result.
If the battery will not be used normally with SOC levels below 10 %, the procedure of slow-rate discharging and resting can also be omitted in order to save time. The significance of extracting the last available charge out of the battery can be mainly seen if the battery is totally discharged. Erroneous capacity results in notable error in the voltage only during the steep OCV slope at the

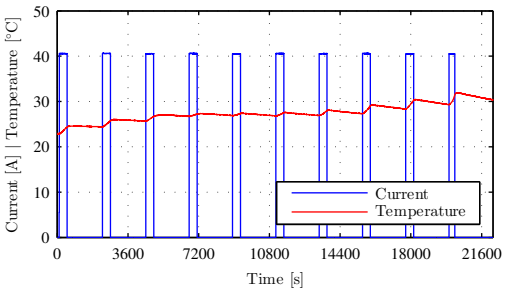

(a) Measured discharge current and temperature.

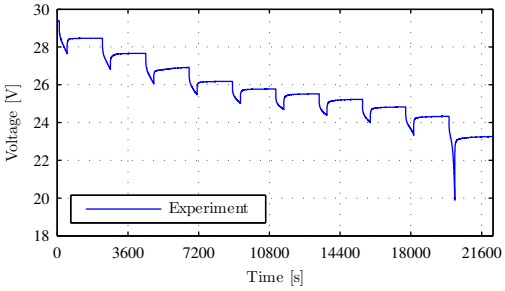

(b) Voltage response.

Figure 2: Typical PD experiment at 1C rate with 10 % pulse rate, and 30 min rest time.

very end of the discharge, i.e., at very low SOC levels.
If the battery characterization must be done in minimum time, the capacity can also be determined from the PD experiments. The downside is that the normal PD experiment's end-of-test criteria is met when the voltage hits the end-of-discharge voltage for the first time. Thus, the residue charge that could be extracted from the battery after the relaxation effect is over is missed. However, after the first PD experiment, it is possible to further continue the discharging. The actual measured capacity should then be used as the nominal capacity in the calculation of the usable capacity in (1).

3.2.2 Open-circuit voltage

The easiest method to characterize the OCV is to make a PD experiment with at least 10 current pulses and long enough rest times for the OCV to achieve steady-state condition, or at least get to near steady-state condition. In [8], it was shown that the relaxation time is in the order of hours, and at a low SOC, the relaxation time still increases significantly. However, the longer relaxation time near the depletion of a battery is significant only if the battery operates regularly at a very low SOC region, and especially, stays there long times without loading. If that kind of operation is likely and that behavior needs to be modeled, either very long rest times at a low SOC region or a rapid test method described in [8] should be utilized. Otherwise, the significant prolonging of the relaxation time does not need specific measures. Worth notice is also that the rest time obviously needs not to be constant for every current pulse, but the length may vary as a function of SOC. That is, the very last pulses at a low SOC may employ longer rest times than the rest of the pulses.
Once the SOC–OCV mapping has been obtained from the experiment, the result may be represented as a LUT with linear interpolation, or as a mathematical function, e.g. polynomial function. However, the problem with using a polynomial function is that the order of the function gets easily high, which yields to a high uncertainty of the parameters, and thus, to poor result. On the other hand, the problem with a low-order polynomial function is that it cannot represent the OCV curve accurately. Therefore, usually the best result is achieved by representing the SOC–OCV mapping as a LUT with linear interpolation.

3.2.3 Ohmic resistance

At the time instants when a new discharge pulse is beginning, the direct voltage drop is due to the ohmic resistance R_0. That is:

$$R_0 = \frac{\Delta U}{\Delta I} \tag{16}$$

The resistance can be calculated at either or both edge of each discharge pulse. This is illustrated in Fig 3, which shows a part of a voltage response for C/2 pulse discharge experiment. The data points for ΔU extraction are shown as red circles, and they are shown at both edges. A LUT or curve fitting can be utilized in order to express the resistance as a function of SOC.

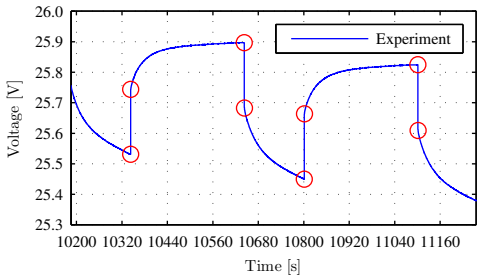

Figure 3: Voltage response for PD experiment. Red circles mark data points for R_0 extraction.

3.2.4 RC parallel circuits

RC-network parameters can be extracted from the voltage data during a current pulse as e.g. in [3, 4, 9]. Another method is to extract the time constants and initial voltages from the voltage data during the rest period. Then, the preceding current-pulse amplitude and duration may be used to extract the resistance and capacitance values. In this way, the measured voltage during the rest period is affected only by the RC-networks. The OCV as well as the values for the

RC branches stay constant during the extraction of the time constants and initial voltages. Also least-squares identification as well as other system identification methods may be used in the parameter extraction.

3.2.5 Self-discharge

The self-discharge rate for lithium-ion batteries is in the area of 5 % per month. This data can be obtained from the manufacturer or by making a dedicated experiment. Obviously, because the self-discharge is a very slow process, the experiment takes weeks. If there is no time for that or long-time simulations are of no interest, the self-discharge behavior can be neglected or the general 5 % per month rate can be used.

3.2.6 Procedure for model extraction

- *Preparation procedures.* After this, the battery is fully charged and balanced and is ready for tests.

- *Characterization of the capacity.* The capacity characterization is needed to determine SOC accurately during the model extraction. For rapid characterization, the capacity can be extracted from the same PD experiments, which are made for the transient response network parameter extraction. Another method is to use constant-current discharging at low rate and to finish the discharging by continuing the discharge after the voltage has recovered because of the relaxation effect until the battery is totally discharged. For a battery with multiple series-connected cells, it must be ensured that none of the cells is discharged below the cut-off voltage. After the experiment is done, the battery should be charged back to full state. Temperature-dependency should also be obtained either by making multiple capacity experiments at different temperatures or by extracting the information from the specification or some other datasheet provided by the manufacturer.

- *Characterization of the OCV.* The OCV can be extracted e.g. with a PD experiment with at least 10 current pulses and long rest times in the order of 30–120 min. After the PD experiment, it is preferred to make also a PC experiment instead of normal charge, because that data can be used afterwards for ohmic resistance and RC parallel branches' parameter extraction as well as model validation. If the OCV from the PC experiment differs notably from that of the PD experiment, average value may be used.

- *Characterization of the ohmic resistance.* The ohmic resistance can be extracted from the PD and PC experiments. The best result is obtained by using a high number of current pulses. Nevertheless, the duration of the experiment can be kept relatively short, because the rest period need not be long. The rest period for obtaining only the ohmic resistance can even be in the order of seconds or tens of seconds. However, for high current rates there may be a need to employ a medium rest period in the area of minutes to cool down the battery. Multiple experiments with various current rates and temperatures should be made to achieve the best result. If there is only very limited time for experiments, the ohmic resistance may also be obtained from the same experimental data that was obtained for the OCV-curve determination.

- *Characterization of the RC branches.* These resistances and capacitances can be obtained from the PD and PC experiments. The experiments should have relatively long rest time in order to be able to characterize also the long time-constant behavior. Generally, the RC network parameters can be extracted from the same experimental data that were obtained from the OCV-curve characterization, if the PD and PC experiments with long rest times were used for that. Otherwise, a new test with rest periods preferably in the area of 10–60 min must be made.

- *Characterization of the self-discharge.* Self-discharge rate can be obtained from the manufacturer or it can be measured. If the model is used only for short-time simulations, the self-discharge behavior can be neglected.

- *Addition of the aging effects.* Aging effects can be added into the model e.g. in the form of LUTs or mathematical expressions. Generally, the capacity degrades and the resistances increase as a function of time and cycles.

3.3 Model evaluation measures

The following error measures are used to evaluate the model: *mean absolute percentage error* (MAPE), and *root mean square percentage error* (RMSPE):

$$\mathrm{MAPE} = \frac{1}{n}\sum_{i=1}^{n}\left|\frac{y_i - \hat{y}_i}{y_i}\right| \times 100 \tag{17}$$

$$\mathrm{RMSPE} = \sqrt{\frac{1}{n}\sum_{i=1}^{n}\left(\frac{y_i - \hat{y}_i}{y_i} \times 100\right)^2} \tag{18}$$

where n is the number of samples, y_i is the i th measured value, and $\hat{y}_i$ is the i th predicted value, i.e. the simulated value.

4 Experimental results

4.1 Test environment

A module-level test environment for battery characterization has been built in the laboratory. Battery modules can be loaded with any current profile up to approximately 500 A discharge and 127 A charge current, respectively. In near future, the laboratory will be upgraded to achieve higher current ratings. Also extra equipment such as temperature chambers will be installed.

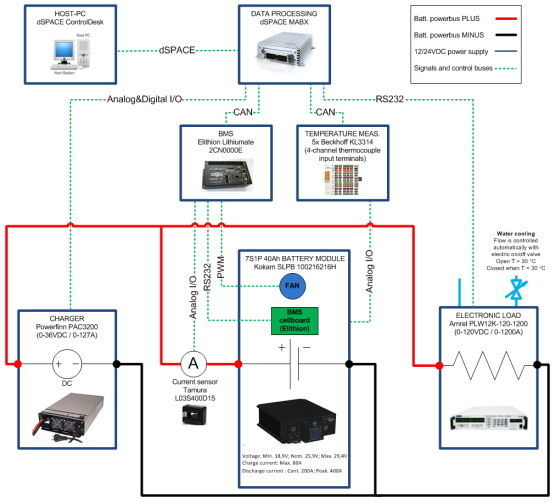

Figure 4: Battery test setup.

A commercial lithium-ion polymer battery module from Kokam was investigated in the experiments. The battery consists of seven series-connected SLPB 100216216H lithium-ion polymer pouch-type cells. The positive electrode material is lithium-manganese-nickel-cobalt-oxide and the negative electrode material is graphite. The specification of the battery is shown in Table 1 and a photo of the battery is shown in Fig. 5.

Table 1: Specification of the battery cell and module.

Property	Unit	Cell	Module
Nominal capacity	Ah	40	40
Nominal voltage	V	3.7	25.9
Max voltage	V	4.2	29.4
Cut-off voltage	V	2.7	18.9
Max charge current	A	80	80
Cont. discharge current	A	200	200
Peak discharge current	A	400	400
Nominal temperature	°C	25	25
Max temp. (charge)	°C	40	40
Max temp. (discharge)	°C	60	60
Cycle life @ 80 % DOD		1 200	1 200

Load current is made with a water-cooled programmable DC electronic load, model PLW12K-120-1200 from Amrel, which has maximum current, voltage, and power ratings of 1 200 A, 120 V, and 12 kW, respectively. A Powerfinn

Figure 5: Battery under test. Additional temperature sensors have been attached inside the module.

PAP3200 is used as a power supply during charging. The power supply can be used as a controlled voltage or current source with output voltage area of 0–36 V and current area of 0–127 A. Its maximum output power is 3.2 kW at 24 V. A Hioki 3390 power analyzer with either a Hioki 9278 or 9279 current clamp—depending on the maximum current of the test—is used to measure current, voltage, power, ampere-hours, and watt-hours.

All equipment except the power analyzer is controlled with a dSPACE *MicroAutoBox* (MABX) DS 1401/1505/1507 rapid control prototyping *electronic control unit* (ECU). Model-based software development is utilized to produce code for the ECU. Models are made with MATLAB/Simulink/Stateflow. The ECU is connected to the host computer via high speed link. All measurements as well as other signals can be monitored online from the host computer through dSPACE ControlDesk software.

All relevant data are logged with 50 ms sampling interval. Data from ControlDesk and power analyzer are merged and postprocessed afterwards to make a unified data structure that has all relevant information for model extraction and validation.

4.2 Model extraction

The capacity of the battery was measured to be approximately 44.7 Ah at room temperature. Manufacturer has also some relative capacity information for elevated as well as colder temperatures. A look-up table was made for $f_3(T)$. The cycle-dependent correction factor $f_1(N)$ and calendar-life dependent correction factor $f_2(t_y)$ were ignored.

Figure 2 shows the measured current pulses, battery average temperature, and voltage response. Based on this experiment, OCV curve (Fig. 6) was extracted at each SOC level. Next, a PD experiment with a rate of C/2, pulse rate of 2 %, and a rest time of 5 min was made (Fig. 7) to obtain a detailed map of the ohmic resistance R_0. The resulting mapping is shown in Fig. 8.

Then, the same experimental data than in the OCV characterization, i.e. Fig. 2, was used to ex-

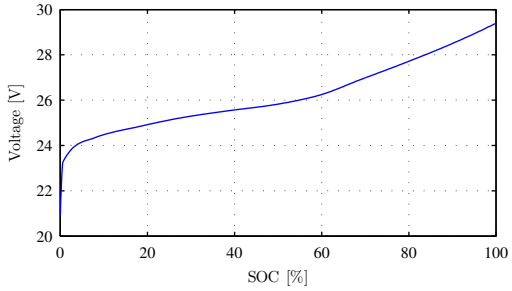

Figure 6: OCV as a function of SOC.

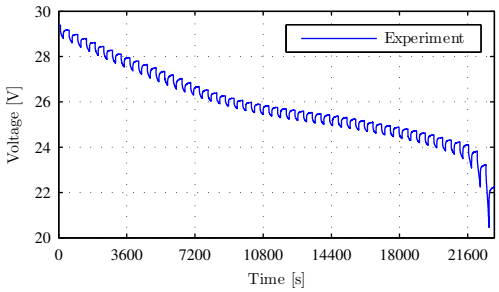

Figure 7: PD experiment at 1C rate, 2 % pulse rate, and 5 min rest periods.

tract the RC parallel circuits' parameters. Simulations were made with three RC-branches to catch the dynamic characteristics at the whole operating area. At very low SOC, the voltage response of the battery starts to slow down rapidly and the the second time-scale resistance increases at the same time. As a consequence, the otherwise almost invisible second time-scale resistance becomes visible. The simulation results of a model are shown in Fig. 9. One part from the middle of the experimented is shown in Fig. 10 to get a better picture of the model accuracy.
As can be seen from the figures, the accuracy of the model is very good. The very short-time peaks in the voltage residual are caused by voltage differences during the current step rise and fall times, the duration of the error peak is only one timestep. They cannot be eliminated by means of parameterizing and they should be neglected in the analysis.

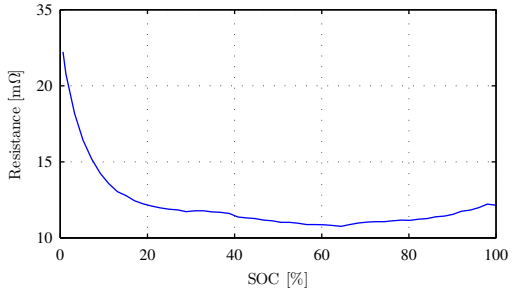

Figure 8: Series resistance as a function of SOC.

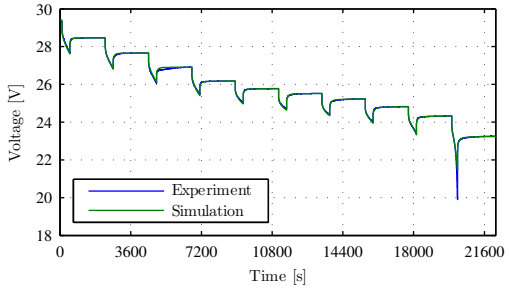

(a) Battery voltage. Simulation result with 3 RC branches.

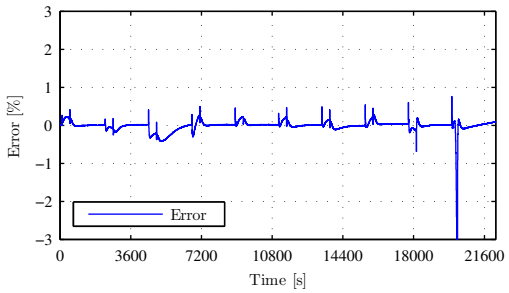

(b) Voltage residual. MAPE = 0.211 %, RMSPE = 0.4949 %.

Figure 9: PD experiment at 1C rate, 10 % pulse rate, and 30 min rest time.

Because battery's charging characteristics are a bit different from discharge characteristics, also a similar charging experiment was made to extract the parameters during charging. However, the charging was finalized with constant-voltage charging instead of constant-current charging.
These experiments were repeated for different current rates to get a relationship between the current-rate and resistance values. The results of the 4C experiment are shown in Fig. 11.

4.3 Model validation

Since there are no standard drive cycles for NRMM, a battery current profile is formed based on a measured power profile of an underground mining LHD loader [10]. The mining loader has a hydrostatic driveline and a hydrostatic implement. The loader was instrumented and test cycles were run in a real test mine. The net power is a sum of traction pump power and implement pump power. An illustration of the duty cycle of the loader and the measured power profile are shown in Fig. 12.
One of many possible electrification schemes is to downsize the ICE and to include a battery as an energy buffer. Because of simplicity, a series-hybrid topology with a battery in the DC link is considered here to form a battery current profile from the measured power profile, see Fig. 13. The ICE is assumed to provide constant power. Thus, the difference between the ICE power and load power is taken from the battery. Therefore, the battery power profile can be obtained

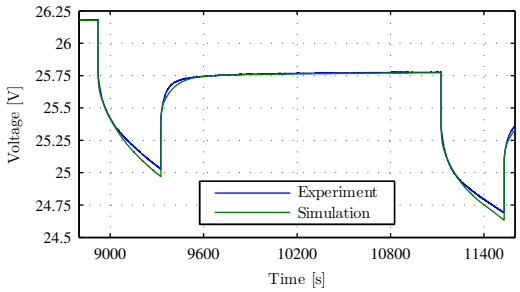

(a) Battery voltage.

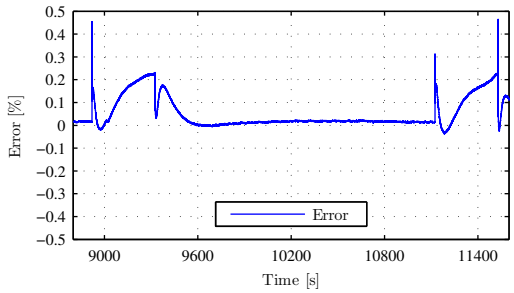

(b) Voltage residual.

Figure 10: Part of experimental PD cycle at SOC around 50 %.

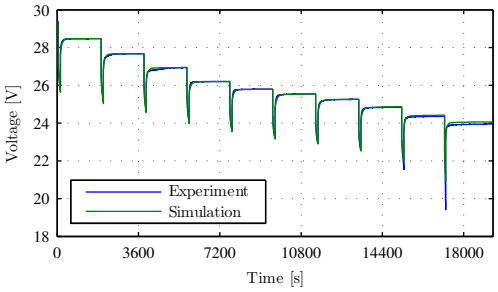

Figure 11: PD experiment at 4C rate, 10 % pulse rate, and 30 min rest time.

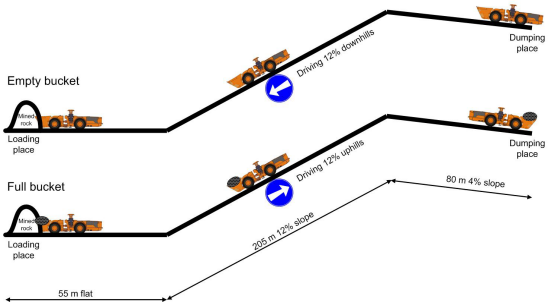

(a) Duty cycle.

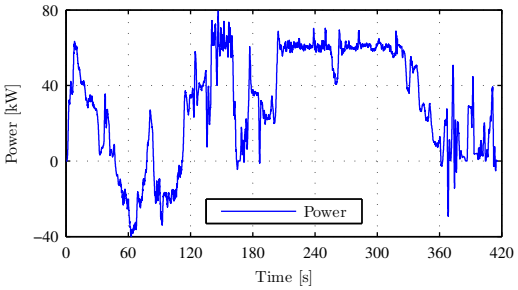

(b) Net power of traction and implement hydraulics.

Figure 12: Duty cycle of an LHD loader. Total length of the cycle is 680 m.

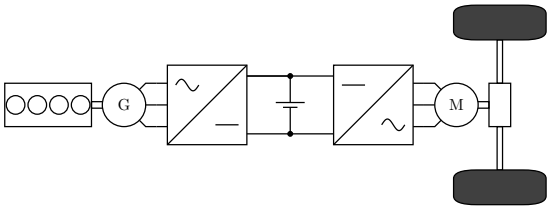

Figure 13: Electrification scheme.

by shifting the total power profile of Fig. 12(b) downwards equally to the engine power. The battery current is then calculated in real-time in the MABX ECU based on the measured module voltage that is multiplied by the number of series-connected modules.

A *charge-depleting* (CD) mode is considered here. Two battery configurations with the same battery module current profile are shown in Table 2. For validation purposes, the whole SOC range is covered. The LHD CD cycle is done so many times that the cut-off voltage is reached, i.e. the first cell reaches the cut-off voltage of 2.7 V.

The results of the experiment and simulation are shown in Fig. 14. As can be seen from the figure, the simulated voltage response follows very closely to the measured voltage in the whole operating area. The higher residual peaks, which occur during instantenous current steps, last only for one sampling period and can be neglected. Thus, the residual of Fig. 14 stays within 1 %. Based on the validation results, it can be concluded that the accuracy of the model is very good, the error is less than 1 % in the normal operation area of 10–100 % SOC and current rate of C/2–4C current-rate. In the experiments, the temperature varied in the range of approximately 23–40 °C, and the temperature effect was included into the model within that range. Better accuracy for the wider temperature range could be achieved by using a temperature chamber or a controlled liquid-cooling system during model parameter extraction process.

5 Conclusion

A versatile battery model for dynamic simulations of EVs and electric NRMM was presented. The model predicts the SOC, OCV, terminal voltage, and SOH for any current profile. It also takes temperature and current rate effects into account in fairly easy and intuitive manner. Calendar life

Table 2: Specification of the battery pack.

Property	Unit	14S2P	28S1P
Modules in series		14	28
Modules in parallel		2	1
Nominal capacity	Ah	80	40
Nominal voltage	V	362.6	725.2
Maximum voltage	V	408.8	817.6
Cut-off voltage	V	264.6	529.2
Maximum charge current	A	160	80
Cont. discharge current	A	400	200
Peak discharge current	A	800	400
Energy	kWh	30	30

and cycle life effects can also be easily included into the model. The model is computationally light, but still the error is within 1 %.
A commercial lithium-ion polymer battery with $LiMnNiCoO_2$ cathode and graphite anode was used in the experiments. The battery consists of seven series-connected 40 Ah pouch-type cells with a nominal voltage of 3.7 V and continuous current rating of 200 A. A module-level laboratory battery test environment was built and used to make experiments and to collect data for model extraction and validation. The model parameters were extracted from a set of simple pulse loading experiments. The model was validated by using a current profile that was formed from a measured power profile of an underground mining loader's typical duty cycle.

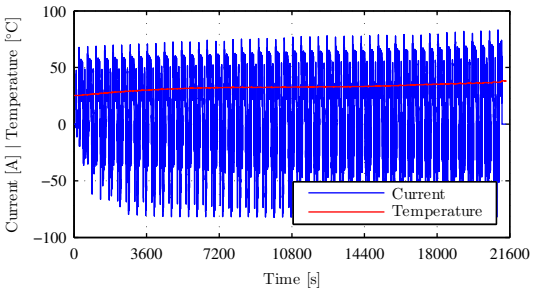

(a) Measured battery current and temperature.

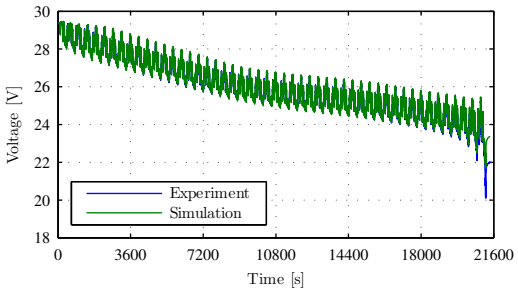

(b) Battery voltage.

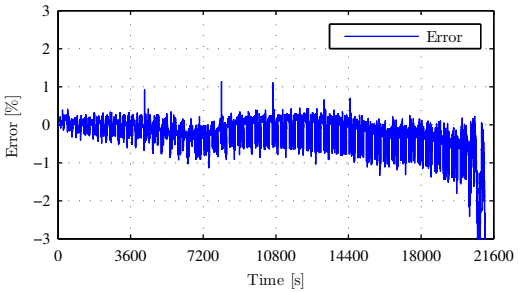

(c) Voltage residual. MAPE = 0.282 %, RMSPE = 0.770 %.

Figure 14: LHD CD experiment.

Acknowledgments

This study has been carried in HybLab project funded by the *Multidisciplinary Institute of Digitalization and Energy* (MIDE) of Aalto University.

References

[1] A. Shafiei, A. Momeni, and S. S. Williamson, "Battery modeling approaches and management techniques for plug-in hybrid electric vehicles," in *Proc. IEEE Veh. Power and Propulsion Conf.*, Chicago, IL, Sep. 2011.

[2] M. Chen and G. A. Rincón-Mora, "Accurate electrical battery model capable of predicting runtime and *I-V* performance," *IEEE Trans. Energy Convers.*, vol. 21, no. 2, pp. 504–511, 2006.

[3] B. Schweighofer, K. M. Raab, and G. Brasseur, "Modeling of high power automotive batteries by the use of an automated test system," *IEEE Trans. Instrum. Meas.*, vol. 52, no. 4, pp. 1087–1091, 2003.

[4] M. Einhorn, V. F. Conte, C. Kral, J. Fleig, and R. Permann, "Parameterization of an electrical battery model for dynamic system simulation in electric vehicles," in *Proc. IEEE Veh. Power and Propulsion Conf.*, Lille, France, Sep. 2010.

[5] N. Watrin, D. Bouquain, B. Blunier, and A. Miraoui, "Multiphysical lithium-based battery pack modeling for simulation purposes," in *Proc. IEEE Veh. Power and Propulsion Conf.*, Chicago, IL, Sep. 2011.

[6] H. Zhang and M.-Y. Chow, "Comprehensive dynamic battery modeling for PHEV applications," in *Proc. IEEE Power and Energy Society General Meeting*, Minneapolis, USA, Jul. 2010.

[7] G. F. Franklin, J. D. Powell, and M. L. Workman, *Digital Control of Dynamic Systems*, 3rd ed. Menlo Park, CA: Addison-Wesley, 1997.

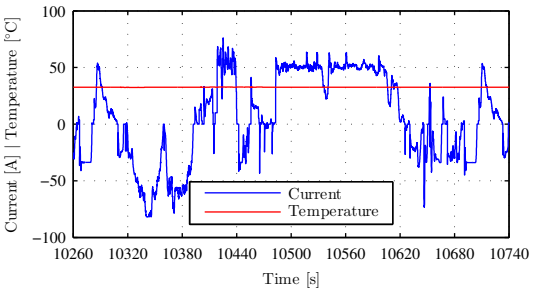

(a) Measured battery current and temperature.

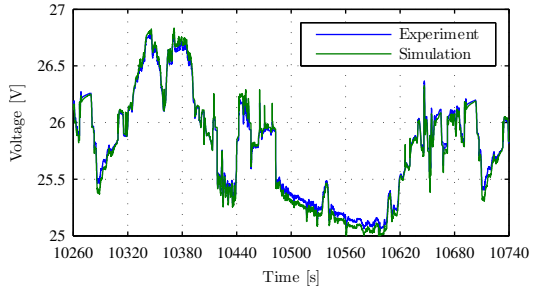

(b) Battery voltage.

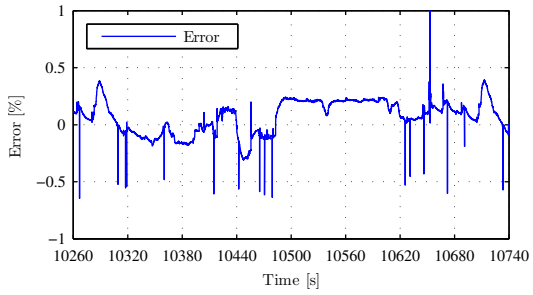

(c) Voltage residual. MAPE = 0.141 %, RMSPE = 0.162 %.

Figure 15: LHD CD duty cycle, zoomed to show details during one cycle in the middle of the experiment.

[8] S. Abu-Sharkh and D. Doerffel, "Rapid test and non-linear model characterisation of solid-state lithium-ion batteries," *J. Power Sources*, vol. 130, pp. 266–274, 2004.

[9] M. Einhorn, V. Conte, C. Kral, and J. Fleig, "Comparison of electrical battery models using a numerically optimized parameterization method," in *Proc. IEEE Veh. Power and Propulsion Conf.*, Chicago, IL, Sep. 2011.

[10] T. Lehmuspelto, M. Heiska, A. Leivo, and A. Hentunen, "Hybridization of a mobile work machine," *World Electric Vehicle Journal*, vol. 3, 2009. [Online]. Available: http://www.evs24.org/wevajournal/

Authors

Ari Hentunen
Ari Hentunen received his M.Sc. (Tech.) degree in electrical engineering from the Helsinki University of Technology (TKK), Finland, in 2005. Currently he is working as a researcher at the Aalto University, Department of Electrical Engineering. His main research interests are modeling of lithium-ion batteries and control of hybrid electric vehicles.

Teemu Lehmuspelto Teemu Lehmuspelto received his M.Sc. degree in mechanical engineering from Helsinki University of Technology (TKK) in 2001. He has been working as a R&D Engineer 2001-2008 in Patria Land & Armament Oy and as a Research Scientist since 2008 in Aalto University. His main research interests are vehicle control technologies and hybrid electric vehicle technologies.

Jussi Suomela Jussi Suomela received the M.Sc., Lic.Sc., and D.Sc. degrees from Helsinki University of Technology (TKK), Espoo, Finland, in 1992, 2001 and 2004, respectively. Suomela has worked in the University since 1991 in various positions. His main research areas are hybrid electric transmission in off-road mobile machines and field and service robotics. At the moment Suomela is professor of automation technology.